Supporting information for

III-VI van der Waals heterostructures for sustainable energy related applications

Jianhui Chen[1], Xiaojun He[1], Baisheng Sa[1,*], Jian Zhou[2], Chao Xu[3], Cuilian Wen[1], and Zhimei Sun[2,**]

[1]*Key Laboratory of Eco-materials Advanced Technology, College of Materials Science and Engineering, Fuzhou University, Fuzhou 350108, P. R. China*

[2]*School of Materials Science and Engineering, and Center for Integrated Computational Materials Science, International Research Institute for Multidisciplinary Science, Beihang University, Beijing 100191, P. R. China*

[3]*Xiamen Talentmats New Materials Science & Technology Co., Ltd., Xiamen 361015, P. R. China*

*To whom the correspondence should be addressed: bssa@fzu.edu.cn.

**To whom the correspondence should be addressed: zmsun@buaa.edu.cn.

Table S1. The lattice constants a (Å), the M-X (M = In, Ga and X = S, Se, Te) bond length L (Å), band gaps E_g (eV) and work functions W (eV) for MX monolayers

System	Functional	a (Å)	$L_{M\text{-}X}$ (Å)	$L_{M\text{-}M}$ (Å)	E_g (eV)	W (eV)
InS	PBE	3.938	2.377	2.820	1.68	
	OptB86-vdW	3.890	2.556	2.801	1.84	
	DFT-D2	3.807	2.533	2.785	2.22	
	HSE06@optB86				2.50	5.65
InSe	PBE	3.965	2.582	2.728	1.72	
	OptB86-vdW	4.029	2.670	2.785	1.75	
	DFT-D2	3.830	2.595	2.683	2.09	
	HSE06@optB86				2.48	5.31
InTe	PBE	4.250	2.820	2.720	1.69	
	OptB86-vdW	4.315	2.866	2.774	1.77	
	DFT-D2	4.107	2.783	2.671	1.91	
	HSE06@optB86				2.34	4.91
GaS	PBE	3.546	2.320	2.412	2.36	
	OptB86-vdW	3.604	2.357	2.460	2.56	
	DFT-D2	3.504	2.305	2.377	2.58	
	HSE06@optB86				3.35	5.40
GaSe	PBE	3.821	2.359	2.473	1.82	
	OptB86-vdW	3.788	2.492	2.458	1.96	
	DFT-D2	3.746	2.474	2.434	2.24	
	HSE06@optB86				2.66	5.13
GaTe	PBE	4.018	2.534	2.399	1.57	
	OptB86-vdW	4.091	2.691	2.454	1.59	
	DFT-D2	3.950	2.616	2.360	1.68	
	HSE06@optB86				2.22	4.98

Table S2. The total energy E_i (eV) for different stacking configurations for MX vdW heterostructures via optB86-vdW

System	Ⅰ	Ⅱ	Ⅲ	Ⅳ	Ⅴ
InSe/GaTe	-25.9134	-25.8202	-25.9210	-25.8200	-25.9151
InS/GaSe	-29.9211	-29.8400	-29.9248	-29.8402	-29.9252
InSe/GaS	-29.7762	-29.7011	-29.7790	-29.7005	-29.7748
InS/GaTe	-27.6581	-27.5642	-27.6640	-27.5639	-27.6612
InTe/GaS	-27.1635	-27.0837	-27.1670	-27.0834	-27.1596
InTe/GaSe	-25.5731	-25.4825	-25.5800	-25.4822	-25.5708
InSe/GaSe	-27.9722	-27.8920	-27.9770	-27.8915	-27.9726
InS/GaS	-31.8281	-31.7509	-31.8300	-31.7502	-31.8279
InTe/GaTe	-23.8201	-23.7201	-23.8280	-23.7200	-23.8194
InS/InSe	-27.5716	-27.4628	-27.5820	-27.4622	-27.5790
InS/InTe	-25.2815	-25.1839	-25.2870	-25.1834	-25.2817
InSe/InTe	-23.6629	-23.5707	-23.6650	-23.5703	-23.6623
GaS/GaSe	-32.4103	-32.2887	-32.4330	-32.2951	-32.4267
GaS/GaTe	-29.7565	-29.6768	-29.7590	-29.6766	-29.7549
GaSe/GaTe	-28.0381	-27.9677	-28.0395	-27.9677	-28.0382

Table S3. The calculated parameters of InSe/GaTe and InS/GaSe heterostructures with different stacking configurations via optB86-vdW

System	parameter	Ⅰ	Ⅱ	Ⅲ	Ⅳ	Ⅴ
InSe/GaTe	a(Å)	4.068	4.063	4.077	4.062	4.070
	d(Å)	3.250	3.926	3.097	3.929	3.229
	$d_{\text{In-In}}$(Å)	2.790	2.785	2.790	2.787	2.784
	$d_{\text{In-Se}}$(Å)	2.678	2.681	2.682	2.681	2.682
	$d_{\text{Ga-Ga}}$(Å)	2.454	2.454	2.455	2.455	2.450
	$d_{\text{Ga-Te}}$(Å)	2.685	2.686	2.688	2.686	2.685
	E_g(eV)	0.78	0.78	0.77	0.78	0.77
InS/GaSe	a(Å)	3.834	3.831	3.838	3.829	3.835
	d(Å)	3.072	3.696	2.989	3.710	3.028
	$d_{\text{In-In}}$(Å)	2.789	2.791	2.789	2.790	2.789
	$d_{\text{In-S}}$(Å)	2.539	2.540	2.538	2.538	2.539
	$d_{\text{Ga-Ga}}$(Å)	2.460	2.458	2.459	2.459	2.460
	$d_{\text{Ga-Se}}$(Å)	2.503	2.501	2.503	2.501	2.503
	E_g(eV)	1.10	1.17	1.02	1.17	1.10

Table S4. The calculated parameters of InSe/GaTe and InS/GaSe heterostructures with different stacking configurations via GGA-PBE.

System	parameter	Ⅰ	Ⅱ	Ⅲ	Ⅳ	Ⅴ
InSe/GaTe	a(Å)	4.002	3.994	4.011	3.997	4.002
	d(Å)	3.145	3.884	2.932	3.869	3.070
	ΔE(meV)	7.88	88.78	0	89.48	6.01
	$d_{\text{In-In}}$(Å)	2.735	2.734	2.737	2.734	2.734
	$d_{\text{In-Se}}$(Å)	2.640	2.638	2.643	2.638	2.639
	$d_{\text{Ga-Ga}}$(Å)	2.398	2.401	2.401	2.397	2.402
	$d_{\text{Ga-Te}}$(Å)	2.639	2.638	2.640	2.637	2.638
	E_g(eV)	0.94	0.87	0.79	0.87	0.86
InS/GaSe	a(Å)	3.773	3.769	3.778	3.769	3.776
	d(Å)	2.961	3.668	2.832	3.669	2.878
	ΔE(meV)	4.47	70.57	2.70	71.64	0
	$d_{\text{In-In}}$(Å)	2.736	2.733	2.735	2.735	2.735
	$d_{\text{In-S}}$(Å)	2.503	2.504	2.506	2.504	2.505
	$d_{\text{Ga-Ga}}$(Å)	2.407	2.409	2.409	2.409	2.408
	$d_{\text{Ga-Se}}$(Å)	2.460	2.460	2.461	2.460	2.460
	E_g(eV)	1.19	1.26	1.11	1.26	1.11

Table S5. The calculated parameters of InSe/GaTe and InS/GaSe heterostructures with different stacking configurations via DFT-D2.

System	parameter	Ⅰ	Ⅱ	Ⅲ	Ⅳ	Ⅴ
InSe/GaTe	a(Å)	3.904	3.896	3.913	3.896	3.906
	d(Å)	2.935	3.683	2.847	3.695	2.894
	ΔE(meV)	1.20	219.92	0	221.04	1.49
	$d_{\text{In-In}}$(Å)	2.690	2.685	2.689	2.687	2.688
	$d_{\text{In-Se}}$(Å)	2.608	2.609	2.608	2.609	2.607
	$d_{\text{Ga-Ga}}$(Å)	2.353	2.357	2.355	2.355	2.354
	$d_{\text{Ga-Te}}$(Å)	2.601	2.604	2.606	2.602	2.602
	E_g(eV)	1.17	0.95	1.09	0.95	1.17
InS/GaSe	a(Å)	3.687	3.680	3.693	3.680	3.686
	d(Å)	2.759	3.460	2.662	3.460	2.708
	ΔE(meV)	6.69	181.63	3.71	183.31	0
	$d_{\text{In-In}}$(Å)	2.694	2.692	2.692	2.684	2.699
	$d_{\text{In-S}}$(Å)	2.481	2.482	2.479	2.482	2.481
	$d_{\text{Ga-Ga}}$(Å)	2.370	2.369	2.368	2.367	2.363
	$d_{\text{Ga-Se}}$(Å)	2.430	2.428	2.431	2.428	2.427
	E_g(eV)	1.44	1.66	1.36	1.58	1.36

Table S6. The calculated total energy of MX (M_1X_1/M_2X_2, M_1X_1 as the top layer, M_2X_2 as the bottom layer) heterostructures $E^{total}_{M_1X_1/M_2X_2}$ (eV), pristine M_1X_1 monolayers $E^{total}_{M_1X_1}$ (eV), pristine M_2X_2 monolayers $E^{total}_{M_2X_2}$ (eV), and mutually independent M_1X_1 and M_2X_2 monolayers which were fixed in the corresponding heterostructure lattice $E^{total}_{M_1X_1+M_2X_2}$ (eV) via optB86-vdW

System	$E^{total}_{M_1X_1/M_2X_2}$	$E^{total}_{M_1X_1}$	$E^{total}_{M_2X_2}$	$E^{total}_{M_1X_1+M_2X_2}$
InSe/GaTe	-25.921	-12.766	-12.891	-25.641
InS/GaSe	-29.925	-14.597	-15.105	-29.675
InSe/GaS	-29.779	-12.766	-17.184	-29.533
InS/GaTe	-27.664	-14.597	-12.891	-27.389
InTe/GaS	-27.167	-10.743	-17.184	-26.883
InTe/GaSe	-25.580	-10.743	-15.105	-25.300
InSe/GaSe	-27.977	-12.766	-15.105	-27.735
InS/GaS	-31.830	-14.597	-17.184	-31.590
InTe/GaTe	-23.828	-10.743	-12.891	-23.538
InS/InSe	-27.582	-14.597	-12.766	-27.313
InS/InTe	-25.287	-14.597	-10.743	-24.995
InSe/InTe	-23.665	-12.766	-10.743	-23.365
GaS/GaSe	-32.433	-17.184	-15.105	-32.201
GaS/GaTe	-29.759	-17.184	-12.891	-29.507
GaSe/GaTe	-28.040	-15.337	-13.102	-27.778

Table S7. The calculated total energy of MX (M_1X_1/M_2X_2, M_1X_1 as the top layer, M_2X_2 as the bottom layer) heterostructures $E^{total}_{M_1X_1/M_2X_2}$ (eV), pristine M_1X_1 monolayers $E^{total}_{M_1X_1}$ (eV), pristine M_2X_2 monolayers $E^{total}_{M_2X_2}$ (eV), formation energy E_f (meV), mutually independent M_1X_1 and M_2X_2 monolayers which were fixed in the corresponding heterostructure lattice $E^{total}_{M_1X_1+M_2X_2}$ (eV), vdW binding energy E_b^{vdW} (meV/Å^2) , and band gap E_g (eV) via DFT-D2

System	$E^{total}_{M_1X_1/M_2X_2}$	$E^{total}_{M_1X_1}$	$E^{total}_{M_2X_2}$	E_f	$E^{total}_{M_1X_1+M_2X_2}$	E_b^{vdW}	E_g
InSe/GaTe	-35.072	-17.736	-16.911	-425.00	-34.595	-33.18	1.07
InS/GaSe	-37.883	-18.896	-18.612	-374.86	-37.488	-31.01	1.41
InSe/GaS	-37.769	-17.736	-19.994	-38.16	-37.390	-29.98	1.32
InS/GaTe	-36.093	-18.896	-16.911	-286.11	-35.631	-33.27	0.85
InTe/GaS	-35.629	-16.181	-19.994	546.09	-35.182	-32.79	-
InTe/GaSe	-34.737	-16.181	-18.612	55.51	-34.272	-32.49	0.19
InSe/GaSe	-36.665	-17.736	-18.612	-316.53	-36.250	-31.31	1.4
InS/GaS	-39.091	-18.896	-19.994	-200.64	-38.738	-29.05	1.56
InTe/GaTe	-33.533	-16.181	-16.911	-440.96	-33.022	-33.20	0.91
InS/InSe	-37.016	-18.896	-17.736	-383.18	-36.581	-28.66	1.47
InS/InTe	-35.194	-18.896	-16.181	-116.68	-34.695	-33.95	0.3
InSe/InTe	-34.253	-17.736	-16.181	-335.88	-33.739	-33.76	0.79
GaS/GaSe	-38.859	-19.994	-18.612	-252.79	-38.514	-29.10	1.59
GaS/GaTe	-36.671	-19.994	-16.911	234.27	-36.266	-31.17	0.21
GaSe/GaTe	-35.688	-18.612	-16.911	-165.69	-35.253	-32.17	0.85

Table S8. The lattice strain ε (KBar) for upper-layer $\varepsilon_{M_1X_1}$ and bottom-layer $\varepsilon_{M_2X_2}$ of MX monolayers in the corresponding heterostructure lattice for MX (M_1X_1/M_2X_2, M_1X_1 as the top layer, M_2X_2 as the bottom layer) heterostructures

System	$\varepsilon_{M_1X_1}$	$\varepsilon_{M_2X_2}$
InSe/GaTe	-1.02	1.36
InS/GaSe	4.11	-2.67
InSe/GaS	14.26	-12.82
InS/GaTe	-5.01	5.69
InTe/GaS	18.66	-18.37
InTe/GaSe	12.78	-12.66
InSe/GaSe	7.63	-6.80
InS/GaS	10.64	-9.23
InTe/GaTe	4.80	-4.64
InS/InSe	-3.22	4.41
InS/InTe	-9.26	9.73
InSe/InTe	-5.43	5.79
GaS/GaSe	-6.53	7.37
GaS/GaTe	-15.61	15.82
GaSe/GaTe	-8.79	9.15

Table S9. The calculated dielectric constants ε , cell volume Ω and normalized slab polarizability α for MX vdW heterostructures

System	ε_x	ε_z	Ω	α_x	α_z
InSe/GaTe	5.46	1.72	513.56	33.38	17.09
InS/GaSe	4.25	1.66	442.14	26.91	14.03
InSe/GaS	4.37	1.66	439.75	26.98	13.93
InS/GaTe	5.48	1.71	488.20	31.76	16.10
InTe/GaS	9.95	1.70	486.84	34.85	16.00
InTe/GaSe	23.94	1.74	512.88	39.11	17.33
InSe/GaSe	4.65	1.68	467.94	29.22	15.09
InS/GaS	3.92	1.64	414.69	24.59	12.91
InTe/GaTe	5.89	1.73	564.42	37.29	18.97
InS/InSe	4.25	1.67	483.52	29.42	15.49
InS/InTe	10.37	1.72	529.96	38.11	17.61
InSe/InTe	5.62	1.73	558.43	36.53	18.68
GaS/GaSe	4.30	1.65	399.11	24.37	12.53
GaS/GaTe	68.44	1.81	444.46	34.85	15.88
GaSe/GaTe	5.81	1.71	470.90	31.02	15.55

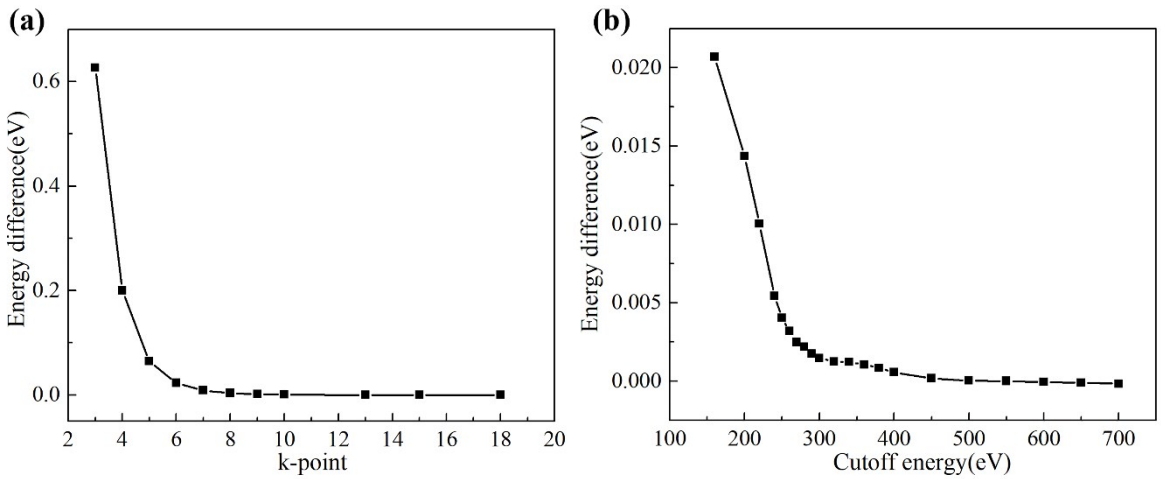

Figure S1. (a)The k-point mesh and (b) cutoff energy convergence test results.

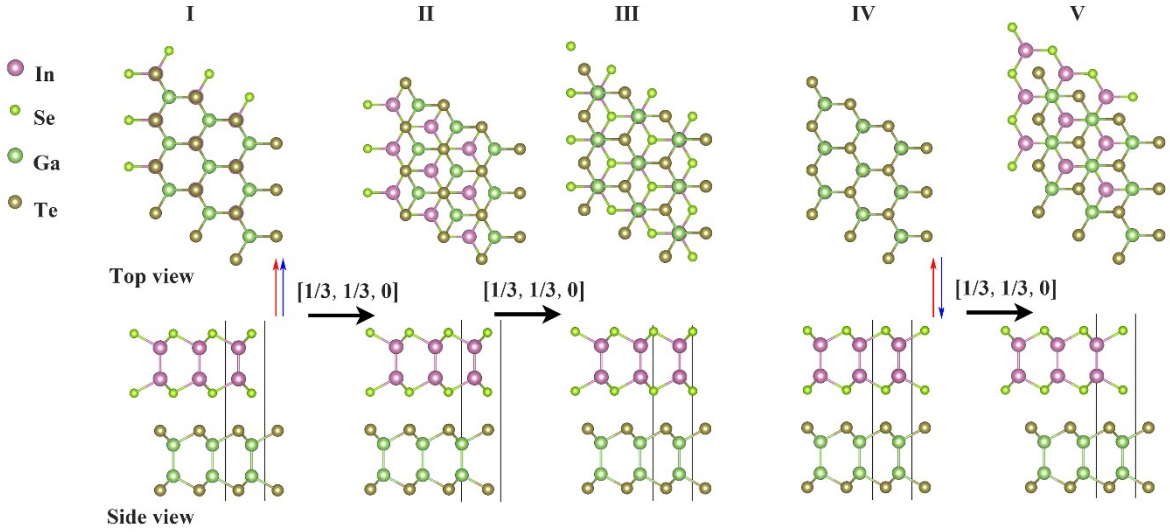

Figure S2. Top and side view of InSe/GaTe heterostructure with five possible stacking configurations.

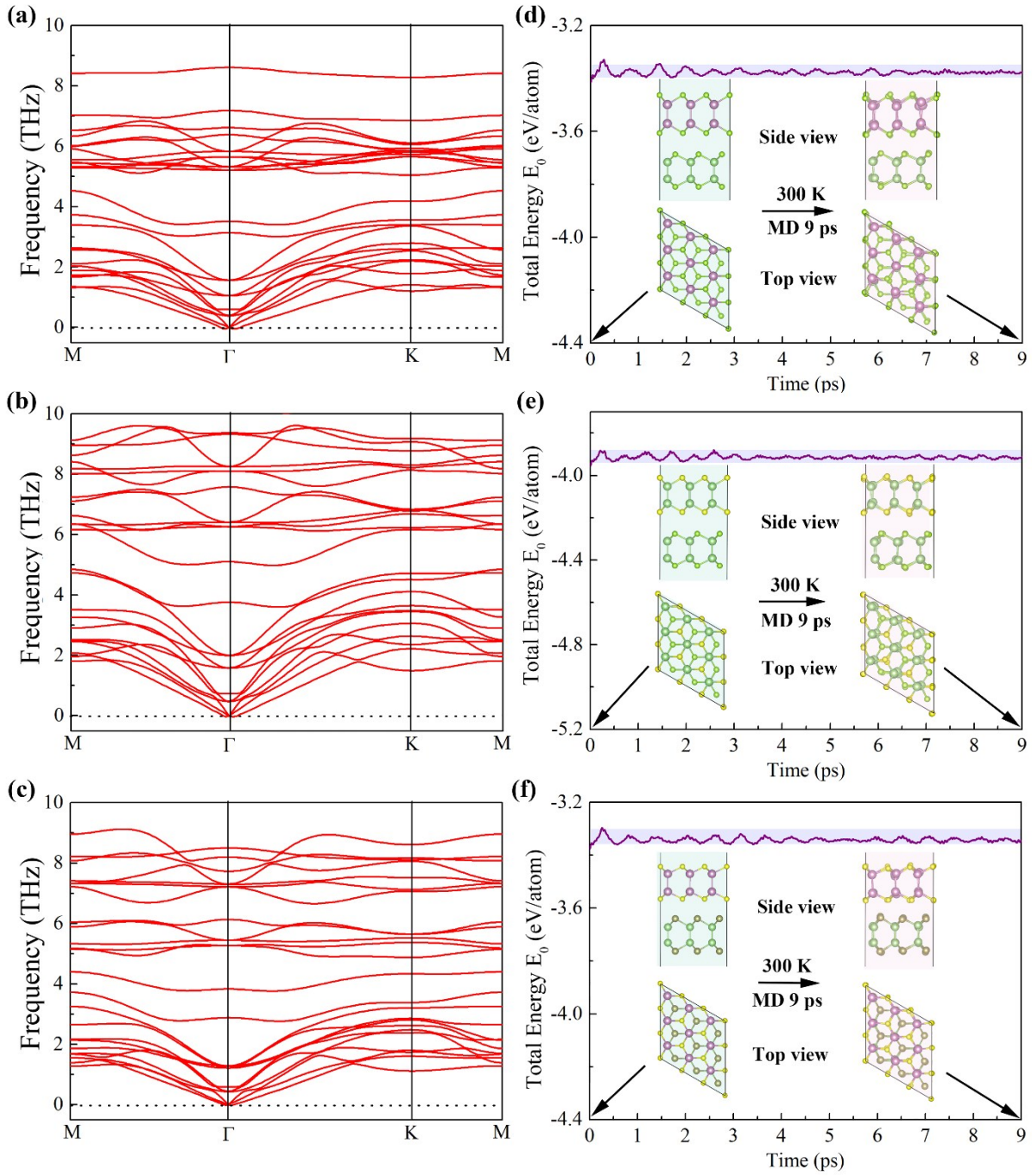

Figure S3. Phonon dispersion curves of (a) InSe/GaSe, (b) GaS/GaSe and (c) InS/GaTe heterostructures. The evolution of total energy of the system in AIMD and snapshots of (d) InSe/GaSe, (e) GaS/GaSe and (f) InS/GaTe heterostructures at 0 ps and 9 ps.

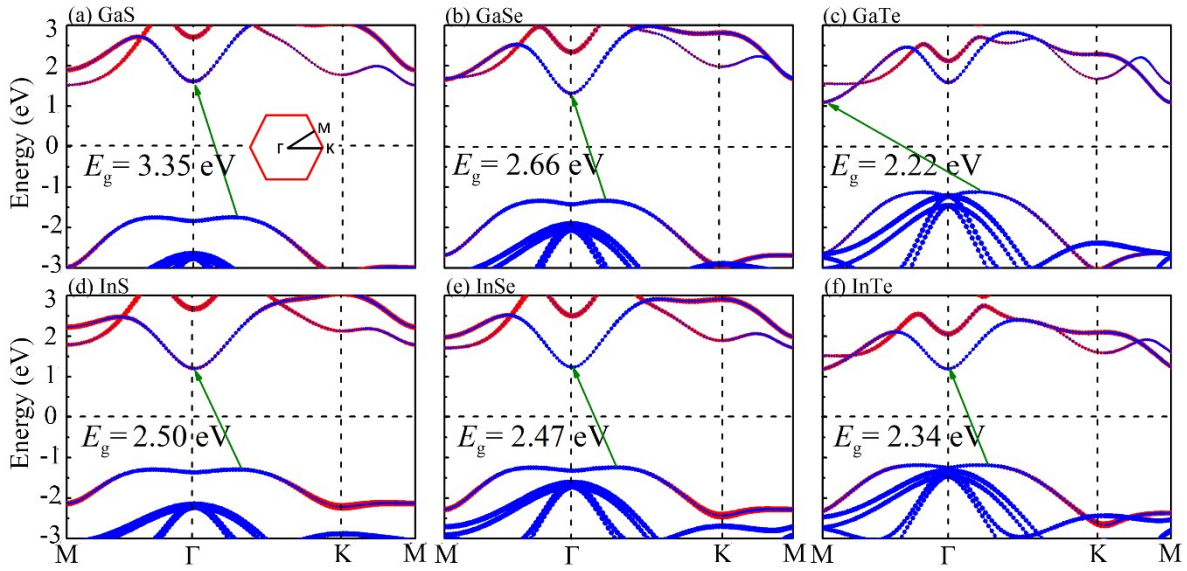

Figure S4. The projected HSE06 band structures of (a) GaS, (b) GaSe, (c) GaTe, (d) InS, (e) InSe and (f) InTe monolayers . The projected weights of *M* and *X* atoms are illustrated by the size of red and blue dots. We set the Fermi level at the center of the band gao as zero reference. The Brillouin zone with high-symmtery points are shown in the inset of (a).

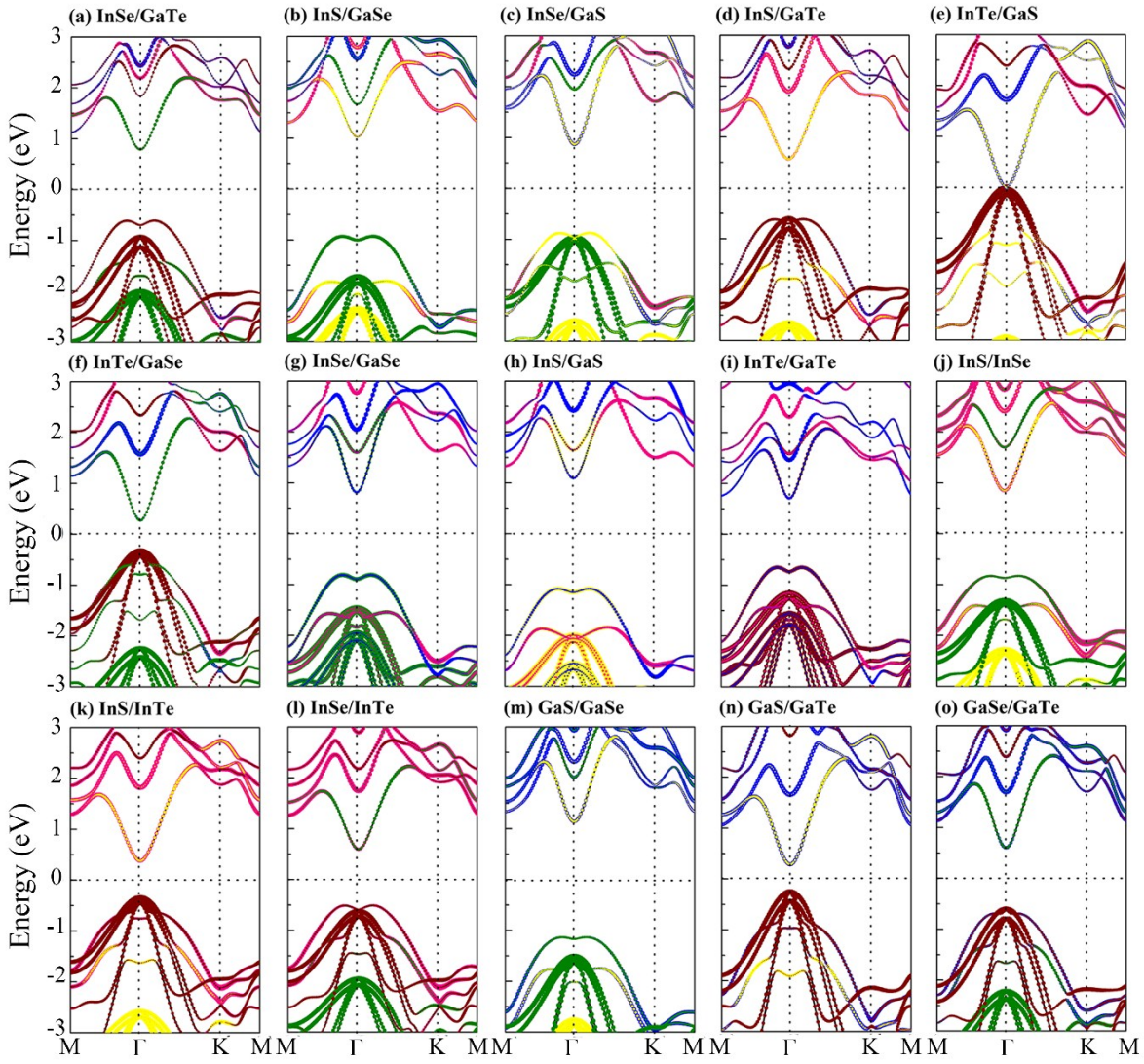

Figure S5. The projected HSE06 band structures of MX vdW heterostructures. The size of blue, pink, yellow, green, and brown circles indicated the projected weight of Ga, In, S, Se, and Te atoms, respectively.

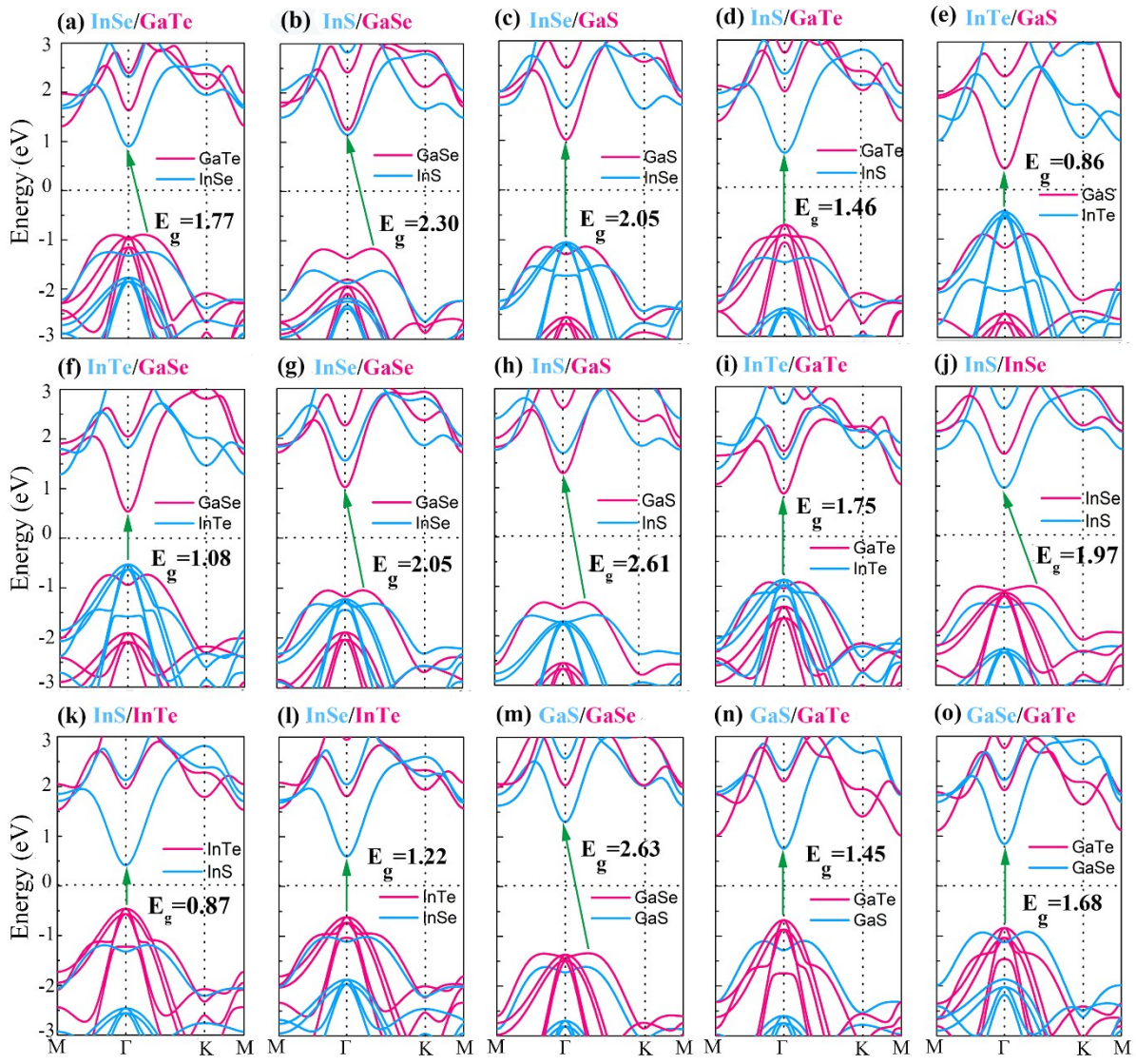

Figure S6. The HSE06 band structures of mutually independent MX monolayers fixed in the corresponding vdW heterostructure lattice.

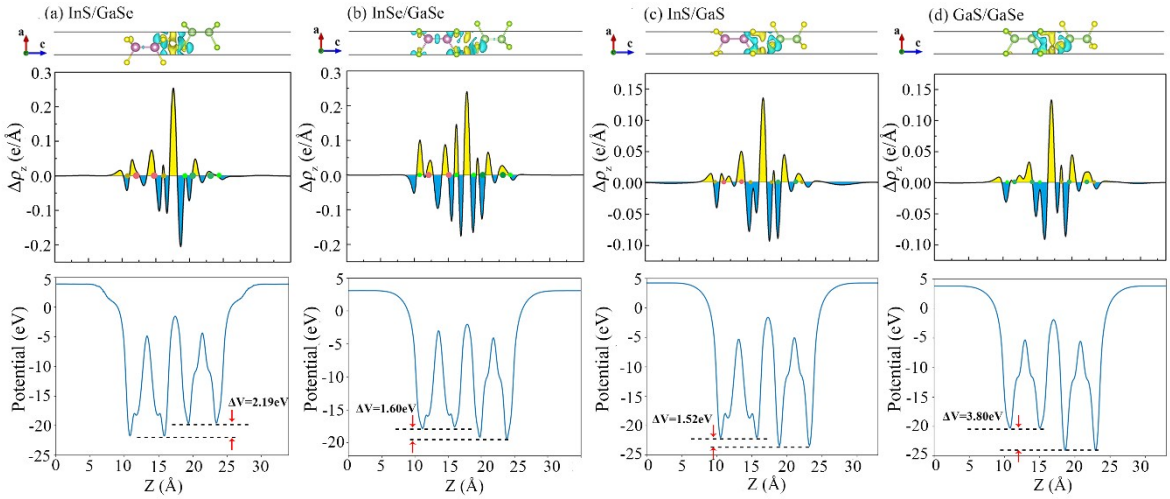

Figure S7. Plane-averaged electron density differnence and plane averaged electronic potential along the direction perpendicular to the vdW interface of (a) InS/GaSe, (b) InSe/GaSe, (c) InS/GaS, and (d) GaS/GaSe heterostructures. The position of atoms are illustrated by the corresponding balls with similar colors, and where the yellow and cyan regions represent the electron accumulation and depletion, respectively.

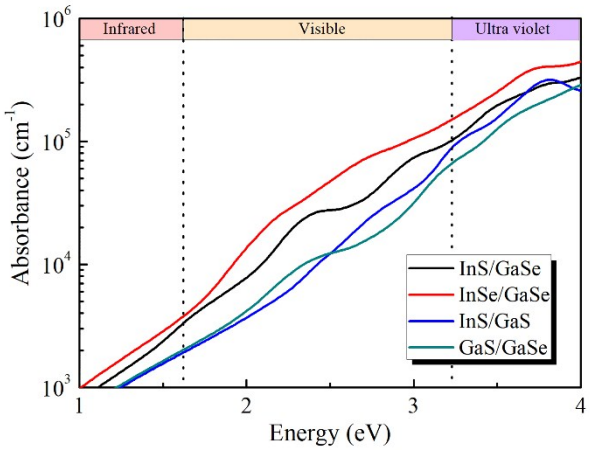

Figure S8. The absorption coefficient α of InS/GaSe, InSe/GaSe, InS/GaS, and GaS/GaSe heterostructures via HSE06 calculations.

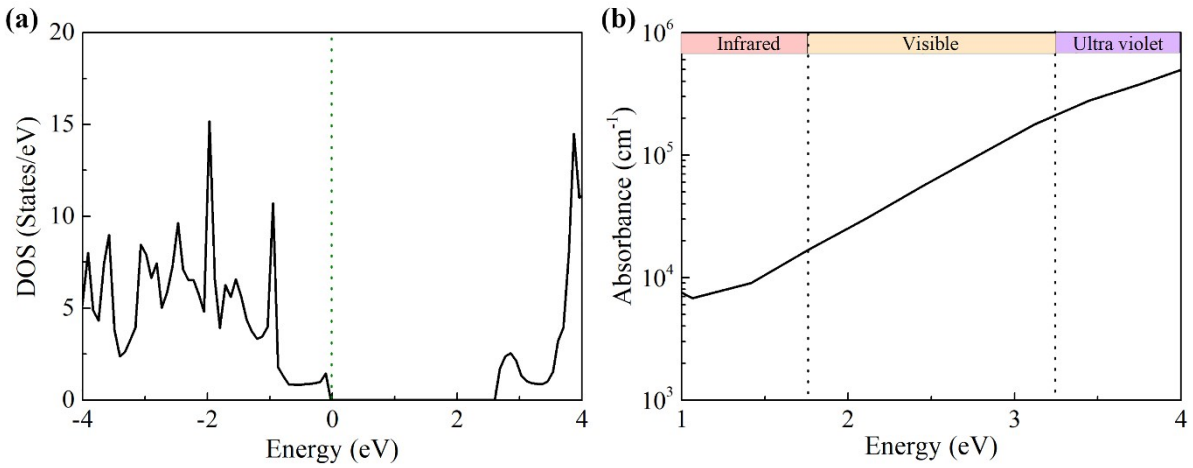

Figure S9. The calculated G_0W_0@HSE06 (a) Total density of states (DOS), and (b) optical absorption coefficients of InS/GaSe heterostructure.

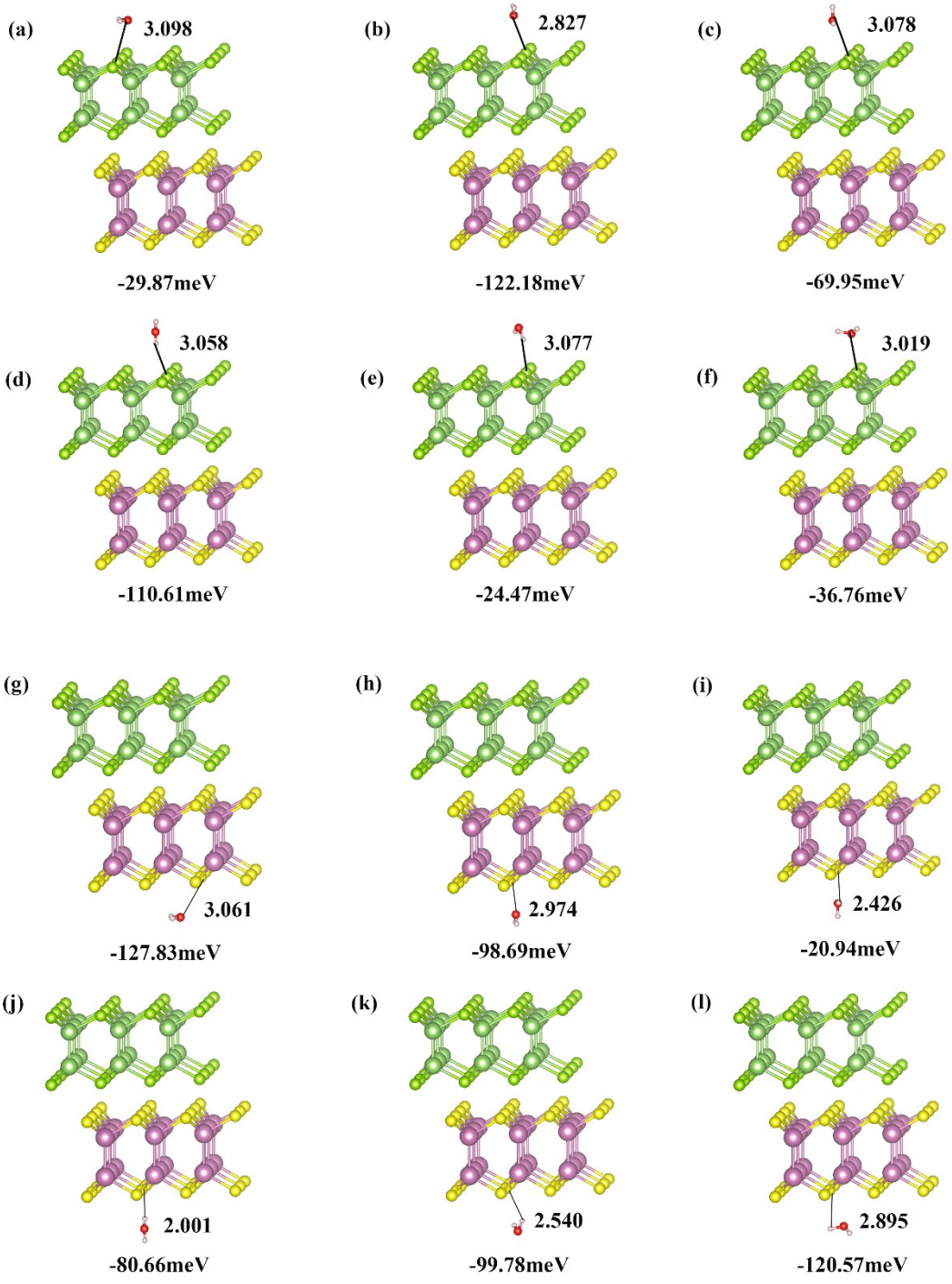

Figure. S10 Optimized structures of water molecule on GaSe and InS surface of InS/GaSe heterostructure with the computed corresponding adsorption energies were shown under the structures.

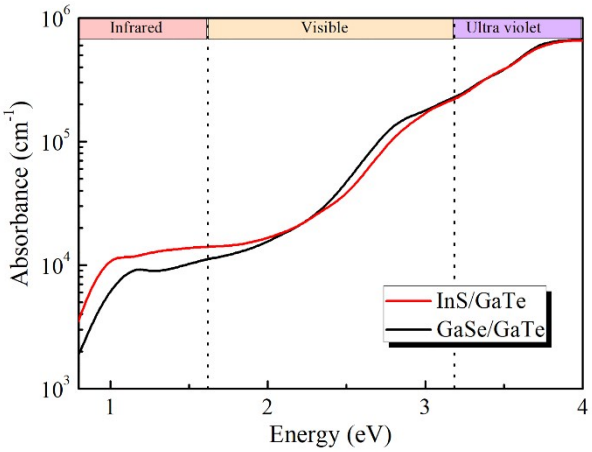

Figure S11. The absorption coefficient α of InS/GaTe and GaSe/GaTe heterostructures via HSE06 calculations.

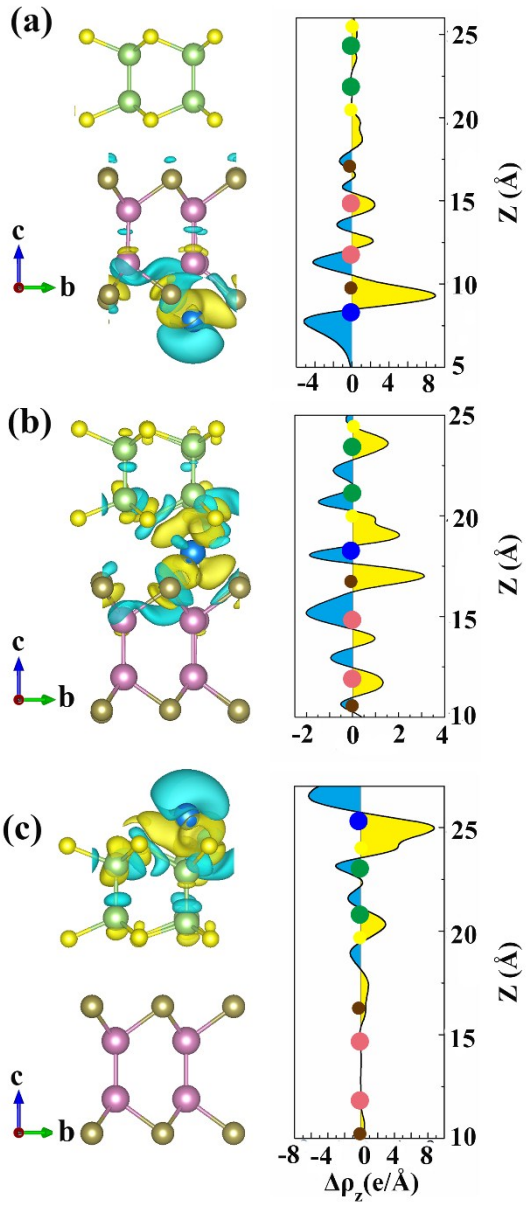

Figure. S12 The charge density difference isosurface and plane-averaged scheme of InTe/GaS heterostructure with one Li ion adsorbed on (a) H_i site, (b) H_m site, (c) H_g site. The loss and gain of electron is illustrated by blue and yellow, respectively.